OPEN ACCESS

# Fabrication of a planar micro Penning trap and numerical investigations of versatile ion positioning protocols

New Journal of Physics
The open-access journal for physics

# Fabrication of a planar micro Penning trap and numerical investigations of versatile ion positioning protocols

**M Hellwig[1], A Bautista-Salvador[1], K Singer[1], G Werth[2] and F Schmidt-Kaler[1,3]**

[1] Institut für Quanteninformationsverarbeitung, Universität Ulm, Albert-Einstein-Allee 11, D-89069 Ulm, Germany
[2] Physikalisches Institut, Johannes-Gutenberg-Universität, 55099 Mainz, Germany
E-mail: ferdinand.schmidt-kaler@uni-ulm.de

*New Journal of Physics* **12** (2010) 065019 (10pp)
Received 8 December 2009
Published 28 June 2010
Online at http://www.njp.org/
doi:10.1088/1367-2630/12/6/065019

**Abstract.** We describe a versatile planar Penning trap structure, which allows one to dynamically modify the trapping configuration almost arbitrarily. The trap consists of 37 hexagonal electrodes, each with a circumcircle diameter of 300 $\mu$m, fabricated in a gold-on-sapphire lithographic technique. Every hexagon can be addressed individually, thus shaping the electric potential. The fabrication of such a device with clean room methods is demonstrated. We illustrate the variability of the device by a detailed numerical simulation of a lateral and a vertical transport and simulate trapping in racetrack and artificial crystal configurations. The trap may be used for ions or electrons, as a versatile container for quantum optics and quantum information experiments.

[3] Author to whom any correspondence should be addressed.

## Contents

1. Introduction 2
2. Versatile trapping configurations and numerical simulations 2
2.1. Single ion trapping . . . . . 3
2.2. Ring crystals and racetrack configuration . . . . . 6
3. Fabrication of the Pixel trap 7
4. Outlook 9
Acknowledgments 9
References 9

## 1. Introduction

Trapped ions have been an important workhorse for quantum information research, even though research has been mostly limited to one-dimensional arrangements of ion crystals in radio frequency Paul traps [1, 2]. Planar Paul traps have shown their advantages for scalable microfabricated devices [3]–[8], even for trapping cold molecules [9]. However, a two-dimensional arrangement of ions [10] still needs to be shown. Inspired by experiments with large, rotating planar ion crystals in Penning traps [11], as well as single ions [12] or electrons [13, 14], novel designs for Penning traps have been proposed [15]–[17]. As an advantage [18], Penning traps operate with only static electric and magnetic fields; thus noise and heating issues as observed for radio frequency ion traps [19] are expected to be largely suppressed. The ac drive of Paul traps, with frequencies from 1 to 100 MHz and with peak-to-peak voltages in the range of a few 100 V, constitutes a considerable source of noise, which affects and heats the trapped particles via free charges and surface patches. The Penning trap, however, even when ions are trapped in the vicinity of slightly contaminated surfaces, is expected to exhibit much better noise properties, as all fields including the patch fields are static.

The static magnetic field lifts the degeneracy of ground state spin states, allowing for a natural choice of qubit basis states. Currently, one of the most urgent unsolved scientific tasks in our field concerns building a scalable quantum information processing device. In this letter we show that novel planar and microstructured Penning traps allow for trapping various qubit configurations, including two-dimensional ion crystals with well-controlled interactions between individual qubits and with individual initialization and readout. Cluster state generation and quantum simulation are future applications of such tailored qubit arrays.

The paper first describes a pixel microstructure to generate the complex electric potential for the novel Penning trap. We briefly sketch the numerical method to calculate the potential landscape with the required high accuracy and optimize the control voltages for a selected set of qubit configurations and qubit operations. We estimate two-qubit spin–spin interactions [20, 21], which would lead either to a multi-qubit cluster state [22] or to the realization of plaquette physics [23] in a rich, however well-controlled, quantum optical few-spin-system. In the last section we show the fabrication of such a device with state-of-the-art clean room technology.

## 2. Versatile trapping configurations and numerical simulations

The genuine three-dimensional Penning trap [13, 14, 44] is composed of a quadrupole electrical potential $\Phi^{\text{el.}}$ provided by a voltage $U$ applied between a ring electrode and two electrically

isolated end cap electrodes of hyperbolic shape, and a superimposed constant magnetic field $B_0$ in the direction of the $z$-axis:

$$\Phi^{\text{el.}}(\rho, z) = \frac{U}{r_0^2}(\rho^2 - 2z^2). \tag{1}$$

The characteristic dimension of the trap electrodes is denoted by $r_0$. The electric field confines charged particles in the axial direction (along the $z$-axis) while the magnetic field prevents them from escaping in the radial direction $\rho$. The motion in this potential consists of three harmonic quantum oscillations at frequencies

$$\omega_\pm = (\omega_c \pm \sqrt{\omega_c^2 - 2\omega_z^2})/2, \tag{2}$$

$$\omega_z = \sqrt{2eU/md^2}, \tag{3}$$

where $\omega_c = eB_0/m$ is the free cyclotron frequency, 400 kHz $T^{-1}$ in the case of $^{40}Ca^+$ ions, which means that in typical experimental settings with singly charged ions [11, 12] one may reach a few MHz of cyclotron frequency. In the case of trapped electrons [13, 14, 24] the cyclotron frequency easily exceeds even 100 GHz. $\omega_+$ is called the reduced cyclotron frequency, $\omega_-$ the magnetron frequency and $\omega_z$ the axial frequency. We note that in the radial direction the ion moves on a potential hill, making the magnetron motion metastable, where the energy of the magnetron motion decreases with increasing quantum number. Axialization, for example by using a rotating electric field (see section 2.1.1), excites the ion, thereby moving it towards the center. The Penning trap stability condition $2\omega_{ax}^2 < \omega_{cyc}^2$ (see e.g. [44]) limits the maximum axial confinement frequency.

In our case the electric field is generated by surface electrodes in one plane [17] instead of the three-dimensional ring structure; see figure 1. Apart from this construction feature, the motional degrees of freedom are similar to those in a three-dimensional Penning trap. In a complex geometry such as our Pixel trap with a large number of different electrodes to control the confinement, see figure 1(a), numerical simulations are used to find a set of voltages for specific tasks and configurations with a few ion qubits. For the shape of the control electrodes, we decided to use a hexagonal shape with a circumcircle diameter of 300 $\mu$m, which allows the formation of spherically symmetric potential field geometries.

In order to obtain accurate electrostatic potentials with minimum numerical noise for our geometry, we apply the fast multipole method for the boundary element problem and calculate the potentials with the exact expressions [40]. Therefore a mesh of $N \sim 12\,446$ surface rectangles is placed on the surface geometry and the surface charges are then obtained in only $O(N)$ steps. As opposed to finite elements or difference methods, only surface elements have to be meshed. When the surface charges for individual voltage configurations are calculated, the potential at any point in space can be obtained by summing over the surface charges weighted by a distance-dependent $1/r$ scaling function.

### *2.1. Single ion trapping*

For an initial trapping of ions, one usually chooses a large trapping volume. To that end all control voltages of the pixels are set to 0 V while the outer four circular segments are at −10 V and the four outermost electrodes at +10 V. The resulting potential exhibits an axial frequency of 500 kHz and a depth of 3.5 eV, ideally suited for trapping, cooling and observing a large cloud; see figure 2.

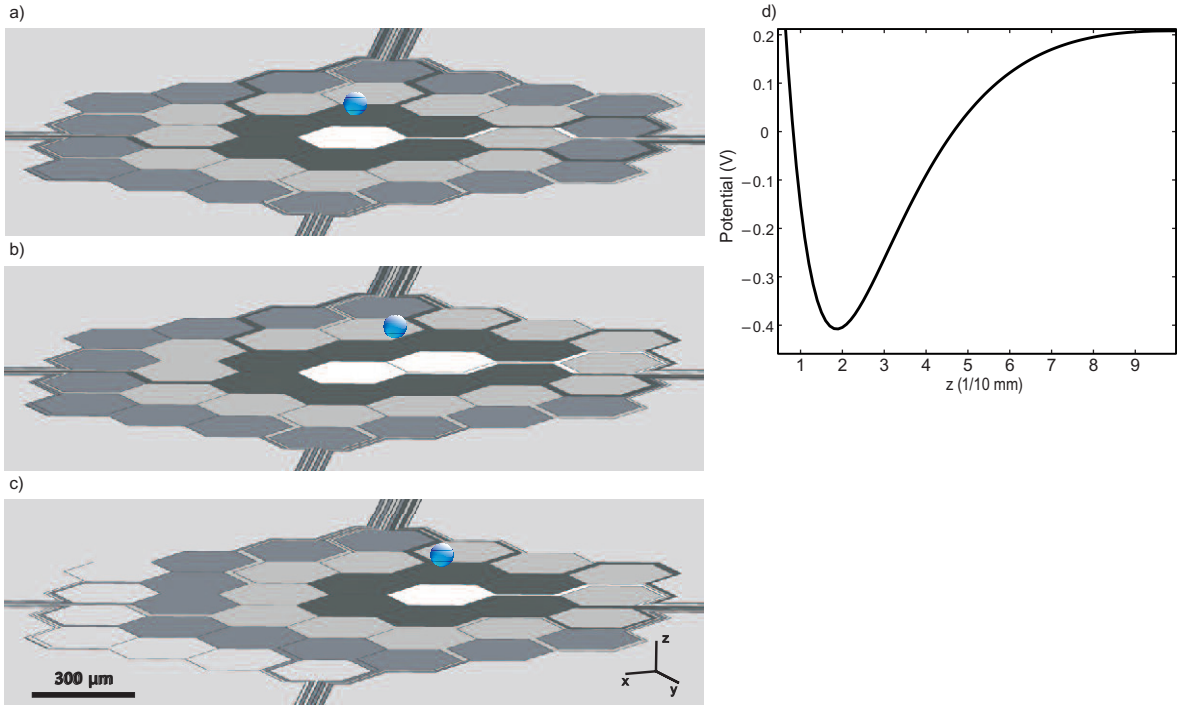


**Figure 1.** (a) Schematics of the Pixel trap for single ion trapping and (b,c) for a lateral transport of an ion by changing of applied potentials. (d) Potential $\Phi_{\mathrm{el}}(z)$ relevant for the axial confinement. If we choose addressing the pixels with 1 V (white), −2.8 V (black), 1 V (light gray) and 3 V (dark gray), we achieve an axial frequency of $\omega_{\mathrm{ax}}/(2\pi) = 1.6$ MHz for calcium ions. The magnetic field points out of the orthogonal to the plane of electrodes.

Starting from this initial setting, the inner electrodes are employed for single ion trapping and we make use of the advanced configurations possible in a Pixel trap. Optimal potentials are obtained by applying regularization techniques [40]. If we supply the voltages 0 V (white), −0.2369 V (black), 1.3171 V (light gray), −28.3125 V (dark gray), 8.1845 V (quartered ring, black) and 10.2997 V (outside plane, gray), see figures 1(a) and 2(a), we would be able to reach a tight trap with an axial frequency of ∼ 1 MHz and a trap depth of ∼ 0.7 eV. The trap minimum is located at a distance of ∼ 0.2 mm from the electrode surface, and the anharmonicities are minimal and only lead to a broadening of the trap frequency well below a kHz for a particle as hot as 5 K. We propose loading and laser-cooling ions in the deep potential (see the previous paragraph) and then altering the voltages to generate a harmonic well.

*2.1.1. Transporting a single ion.* Ions may be transported in the Pixel trap either (i) orthogonal to the plane of electrodes, a transversal transport, or (ii) in a lateral transport parallel to the trap electrode surface. In the case of (i) the pixels are arranged as rings on equal potential, such that the position of the minimum of the axial potential varies [25]. A possible application of a transversal transport would be the determination of motional heating and decoherence rates as a function of ion surface distance, similar to attempts for dynamic Paul traps [26]. The lateral

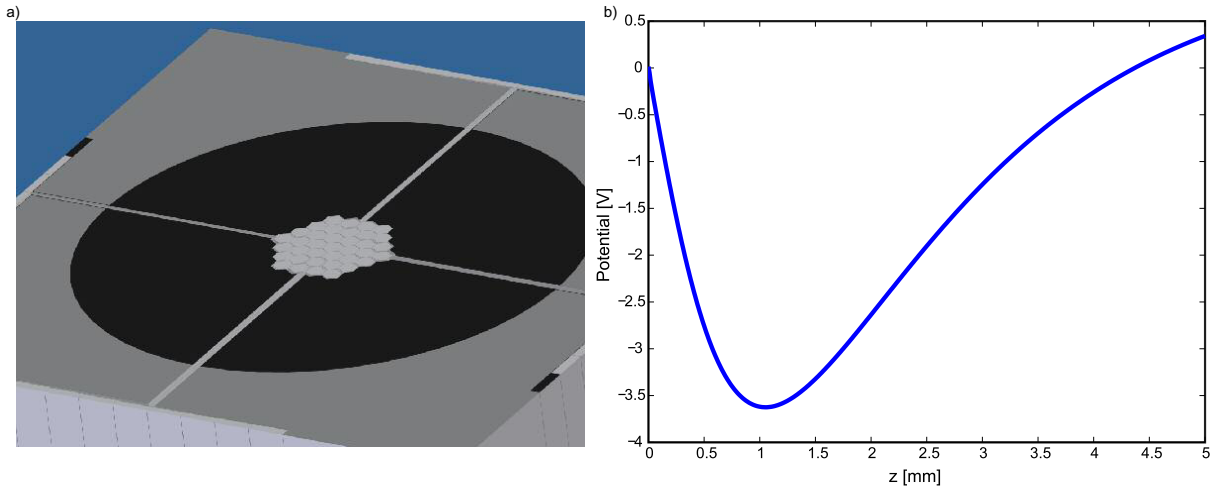


**Figure 2.** (a) Configuration with a large trapping volume and a deep confining potential. All the hexagons are set to 0 V, the quartered ring around it serves as the first ring electrode at −10 V and the rest serves as the outer ring electrode with 10 V. (b) Axial trapping potential.

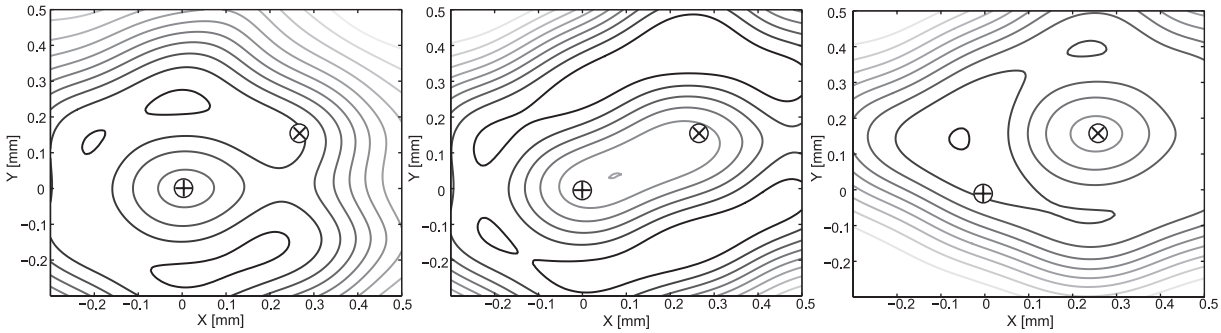


**Figure 3.** $\Phi_{\mathrm{el}}(x, y)$ of the electrode configuration used at the start, in the middle and at the end of the transport, respectively, shown as contour plots. The starting position of the transport is marked with ⊕ and the endpoint with ⊗.

transport is sketched in figures 1(a)–(c) (conceptually) as well as figure 3 (radial potentials). Starting out with a configuration that uses a single pixel as its center, we widen it up to an elongated center, including adjacent pixels, then we tilt the potential in the direction of the new center and finally finish with a single ion confinement at the displaced position. In our scheme, we intend to vary the electric field slowly, such that the much faster cyclotron orbiting can follow adiabatically. Alternatively, for other types of planar Penning traps, it has been proposed [27] to apply a pulsed electric transversal field for a non-adiabatic transport.

The ion is confined near the *maximum* of the radial electric potential $\Phi_{\mathrm{rad}}(x, y)$ as the magnetron oscillation corresponds to an inverted harmonic potential. Axialization, an excitation of the ion's magnetron frequency, centers it to $\Phi_{\mathrm{rad}}^{\mathrm{max}}$. Experimentally, the outer four segments, see figure 2, may be employed to generate a rotating wall potential for this excitation [28].

The lateral transport of single ions may be readily expanded to a joining and splitting operation for two ion crystals, a technique that has so far been limited to segmented linear Paul traps [33]–[35].

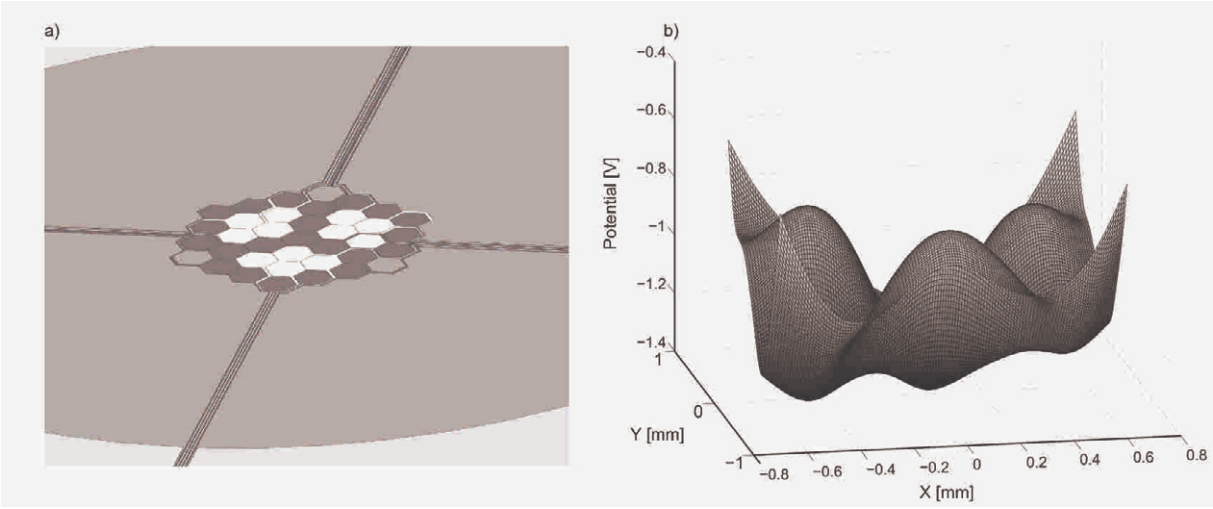


**Figure 4.** (a) Electrode configuration for an artificial ion crystal with three sites. With voltages of 0.6 V (white), −4.0 V (dark gray) and 0.5 V (light gray), we reach a trap depth of 0.8 eV and axial frequencies near 800 kHz. (b) $xy$-potential of the trapping configuration shown in (a), an artificial ion crystal with three ions.

### *2.2. Ring crystals and racetrack configuration*

In a linear Paul trap, typically ions arrange as linear ion strings, while two- or three-dimensional arrangements of ions suffer from micromotion in the dynamical trapping field since the micromotion vanishes only along one line, where the RF field is zero [29, 30]. For crystal sizes on the order of 10 $\mu$m, this motion reaches amplitudes on the order of 1 $\mu$m. Here, a clear advantage of the purely static electric field of a Penning trap becomes evident, because in our geometry two-dimensional 'artificial ion crystals' may be trapped by creating multiple trapping sites. The only relevant motion left in this case is the cyclotron motion, which in the case of an electron in a cryogenic trap (i.e. $T_e \sim 4$ K, see [24]) would have an orbit-radius of $r_{cyc} \sim 15$ nm and in the case of a laser-cooled calcium ion (i.e. $T_{Ca} \sim 1$ mK) a radius of $r_{cyc} \sim 65$ nm[4].

We highlight this with an arrangement of sites around a circle, trapping for example three ions in predefined places. One example of such an electrode configuration is shown in figure 4(a). The potential in the $xy$-plane above such an electrode configuration is displayed in figure 4(b) with three trapping sites. The interest of the Pixel Penning trap is that various different kinds of such configurations may be converted into each other by a time-dependent addressing of the pixel electrodes.

The colloquial term 'racetrack' is commonly used for a configuration in which the trapping zone is in the form of a ring. Radio frequency ion traps have been used to hold linear crystals in a racetrack configuration [31], inspired by confined charged particles in accelerator rings. Magnetic traps with additional radio-frequency fields have been proposed for racetrack configurations for interferometric purposes [32]. Optical potentials for trapping neutral atoms [36, 37] are yet another option. Our Penning trap approach does not require any time-dependent fields, advantageous with regard to heating and decoherence, and technically less demanding. In the Pixel Penning trap we may realize a 580 $\mu$m diameter racetrack; see figure 5.

[4] An ion at room temperature would of course show quite a large cyclotron orbit of $\sim 35$ $\mu$m.

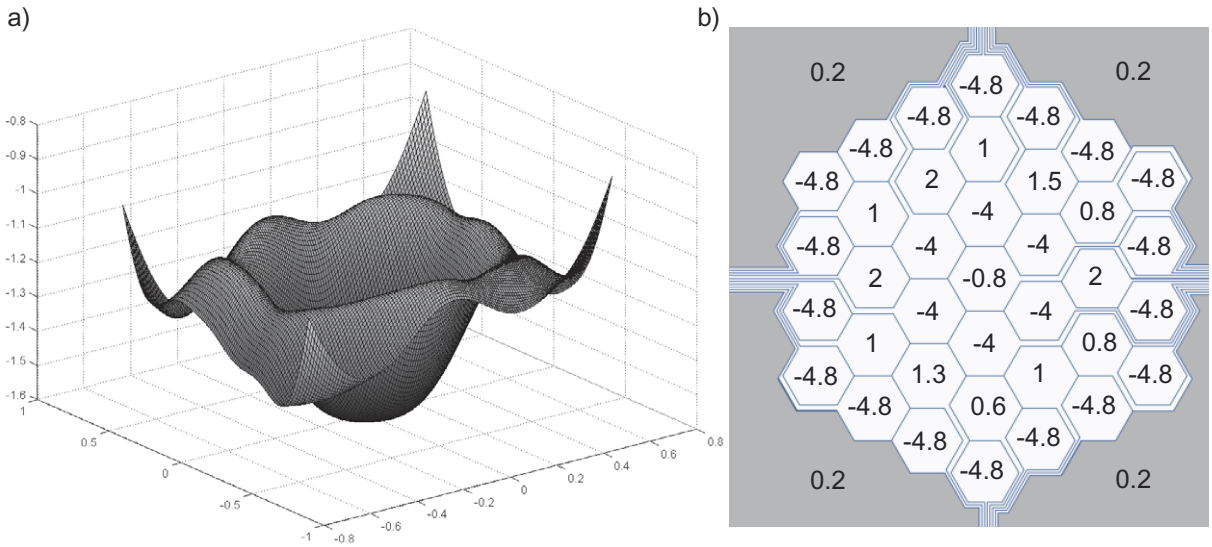


**Figure 5.** (a) Resulting potential $\Phi_{el}(x, y)$ for a racetrack configuration. (b) Map of the voltages needed to create this potential (unit is volts). The differences in the individual voltages on the actual racetrack are due to slightly varying sizes of the pixels.

## 3. Fabrication of the Pixel trap

Starting with the CAD file of the trap design, we realize the fabrication of planar Penning traps by three-step clean room processing: photolithography, electroplating and etching. The fabrication is schematically presented in figure 6. A polished borosilicate glass wafer serves as the substrate. We have achieved similar results with 2′ sapphire wafers of thickness 0.50 mm, which has the advantage of better heat conduction, even at cryogenic temperatures. In order to ensure proper adhesion of the Au electrodes to the substrate, an adhesion promoter layer is mandatory. We use a 5 nm Cr layer deposited on the wafer via thermal evaporation. Furthermore, to enhance Au electrodeposition a 50 nm Au seed layer is also thermally deposited on top and a negative resist[5] is added. Photolithography is then carried out. The mask resist lines that define the gaps between electrodes show a width of 4.0 $\mu$m. Electrodes are grown up to 4.0 $\mu$m in a Au plating bath[6]. This means we achieve an aspect ratio of 1 between the depth and width of the gaps between the electrodes, shielding inter-electrode insulating substrate gaps from the ion position. After electroplating, the resist mask is stripped off. The Au seed layer is removed (using $KI/I_2$ gold etchant) and a final Cr etching step is performed. Figure 7 shows a scanning electron microscopy micrograph of the inner center of the Pixel trap.

We dice the wafers and ball bond the chip electrodes to an 84-pin Kyocera chip carrier using 25 $\mu$m Au wires. Under UHV conditions with $10^{-7}$ mbar, we investigate the limit of the applied electric field by raising slowly the applied voltage. We observe a breakdown at approximately 180 V for 1.2 $\mu$m to 720 V for 4.0 $\mu$m gap width, far above the required trap voltages.

[5] AZ® nLOF 2070.
[6] Mixture of Enthone GRC complex and Enthone microfab Au-100B.

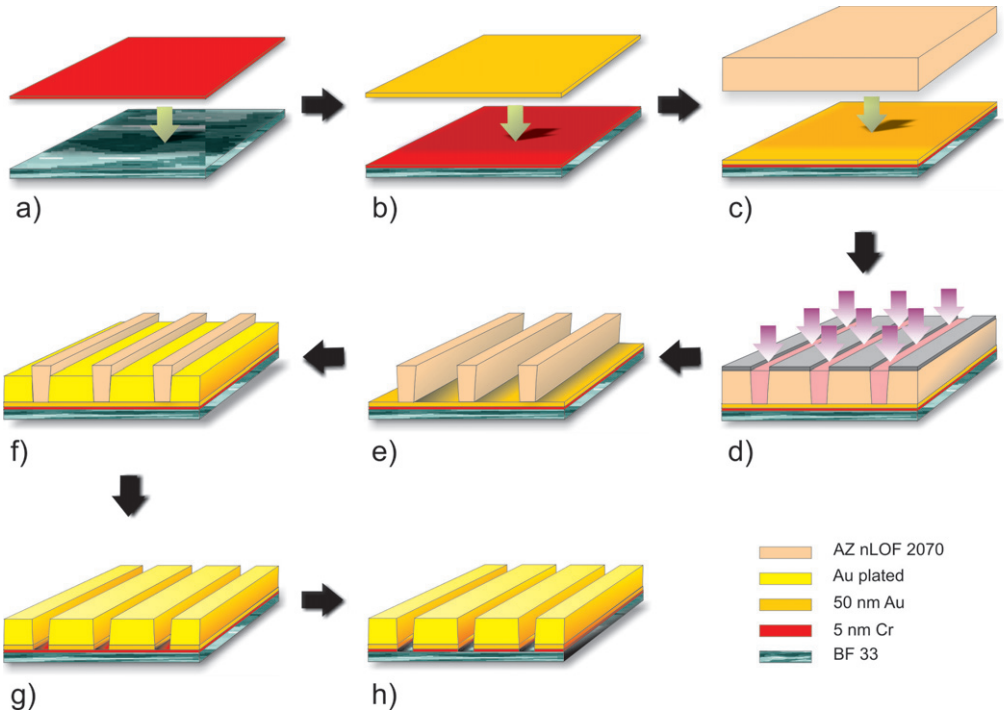


**Figure 6.** Simplified scheme of the fabrication process. (a) Evaporation of the adhesion Cr layer on BF® 33 wafer, (b) evaporation of the starting Au layer on Cr/BF® 33, (c) spin coating of AZ nLOF 2070 resist, (d) photolitography: exposure to UV light, (e) development, (f) electroplating of Au, (g) stripping of resist and wet-etching of Au seed layer and (h) wet-etching of Cr.

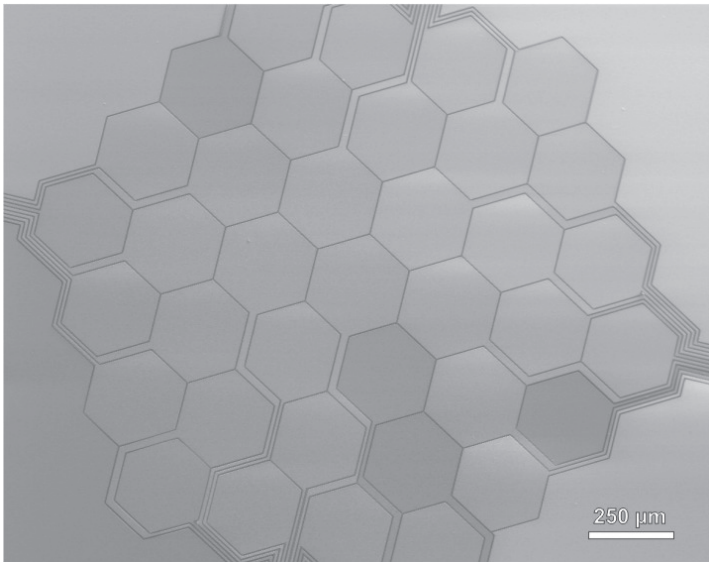


**Figure 7.** SEM micrograph of the gold-on-sapphire Pixel Penning trap.

## 4. Outlook

As a next step, we plan experimental tests with single trapped $^{40}Ca^{+}$ ions in the Pixel trap in order to particularly optimize the control of the transport processes [38, 39]. The Pixel trap opens a way to miniaturized Penning traps, and once the coherence properties have been tested with single ions close to surfaces, one might further reduce the spatial dimensions of the surface electrodes to about 10 $\mu$m, including a dual layer technique [8]. In a planar arrangement of trapped atoms, one may perform entanglement gate operations that are mediated by an inhomogeneous magnetic field [20, 22]. The interaction Hamilton operator $H_{spin} = \hbar/2 \sum_{n<m} J_{nm}\sigma_{z,n}\sigma_{z,m}$ denotes the coupling of two spins, where the strength of the coupling $J_{nm}$ can be controlled by the distance of the atoms and the magnetic gradient field. With ion–ion distances of a few 10 $\mu$m and realistic magnetic gradient fields of 10–50 T m$^{-1}$, one will reach a coupling strength $J_{nm}$ of kHz for the mutual effective spin–spin interaction. We aim for scaling up the number of qubits that participate in the generation of cluster states (see [22] for details) using a two-dimensional instead of a linear ion crystal. Further applications in quantum science would be experimental tests of quantum state transfer protocols [41, 42], which have been proposed but not realized experimentally so far. The two-dimensional ion crystals would also facilitate quantum simulation because the spin–spin distance and the geometry could be controlled by the trapping fields even more flexibly than in the situation of ultra-cold atoms in optical lattices [43].

## Acknowledgments

A B-S thanks CONACYT for financial support through the scholarship ID 206267. We acknowledge financial support by the German science foundation DFG within the SFB/TRR-21, the European commission within MICROTRAP (Contract no 517675) and the excellence program of the Landesstiftung Baden-Württemberg.

## References

[1] Häffner H, Roos C F and Blatt R 2008 *Phys. Rep.* **469** 155
[2] Blatt R and Wineland D J 2008 *Nature* **453** 1008
[3] Madsen M J, Hensinger W K, Stick D, Rabchuk J A and Monroe C 2004 *Appl. Phys.* B **78** 639
[4] Pearson C E, Leibrandt D, Bakr W S, Mallard W J, Brown K R and Chuang I L 2006 *Phys. Rev.* A **73** 32307
[5] Seidelin S *et al* 2006 *Phys. Rev. Lett.* **96** 253003
[6] Leibrandt D, Clark R J, Labaziewicz J, Antohi P, Bakr W S, Brown K R and Chuang I L 2007 *Phys. Rev.* A **76** 55403
[7] Wang S, Labaziewicz J, Ge Y, Shewmon R and Chuang I L 2009 *Appl. Phys. Lett.* **94** 094103
[8] Amini J M, Britton J, Leibfried D and Wineland D J 2008 arXiv:0812.3907
[9] Debatin M, Krner M, Mikosch J, Trippel S, Morrison N, Reetz-Lamour M, Woias P, Wester R and Weidemüller M 2008 *Phys. Rev.* A **77** 033422
[10] Schmied R, Wesenberg J H and Leibfried D 2009 *Phys. Rev. Lett.* **102** 233002
[11] Skiff F, Bollinger J, Jensen M J, Hasegawa T and Bollinger J J 2004 *Phys. Rev.* A **70** 033401
[12] Crick D R, Ohadi H, Bhatti I, Thompson R C and Segal D M 2008 *Opt. Express* **16** 2351
[13] Brown L S and Gabrielse G 1986 *Rev. Mod. Phys.* **58** 233
[14] Hanneke D, Fogwell S and Gabrielse G 2008 *Phys. Rev. Lett.* **100** 120801
[15] Castrejón-Pita J R and Thompson R C 2005 *Phys. Rev.* A **72** 1

[16] Castrejón-Pita J R, Ohadi H, Crick D R, Winters D F A, Segal D M and Thompson R C 2007 *J. Mod. Opt.* **54** 1581
[17] Stahl S, Galve F, Alonso J, Djekic S, Quint W, Valenzuela T, Verdù J, Vogel M and Werth G 2005 *Eur. Phys. J.* D **32** 139–46
[18] Taylor J M and Calarco T 2007 arXiv:0706.1951
[19] Labaziewicz J, Ge Y, Antohi P, Leibrandt D, Brown K R and Chuang I L 2008 *Phys. Rev. Lett.* **100** 13001
[20] Johanning M, Braun A, Timoney N, Elman V, Neuhauser W and Wunderlich Chr 2009 *Phys. Rev. Lett.* **102** 073004
[21] Daniilidis N, Lee T, Clark R, Narayanan S and Häffner H 2009 *J. Phys.* B **42** 154012
[22] Wunderlich H, Wunderlich Chr, Singer K and Schmidt-Kaler F 2009 *Phys. Rev.* A **79** 052324
[23] Paredes B and Bloch I 2008 *Phys. Rev.* A **77** 023603
[24] Bushev P, Stahl S, Natali R, Marx G, Stachowska E, Werth G, Hellwig M and Schmidt-Kaler F 2008 *Euro. Phys. J.* D **50** 97
[25] Marzoli I *et al* 2009 *J. Phys. B: At. Mol. Opt. Phys.* **42** 154010
[26] Deslauriers L, Olmschenk S, Stick D, Hensinger W K, Sterk J and Monroe C 2006 *Phys. Rev. Lett.* **97** 103007
[27] Crick D R, Donnellan S, Ananthamurthy S, Thompson R C and Segal D M 2009 arXiv:0901.2716v1
[28] Powell H F, Segal D M and Thompson R C 2002 *Phys. Rev. Lett.* **89** 093003
[29] Herskind P F, Dantan A, Albert M, Marler J P and Drewsen M 2009 *J. Phys. B: At. Mol. Opt. Phys.* **42** 154008
[30] Berkeland D J, Miller J D, Bergquist J C, Itano W M and Wineland D J 1998 *J. Appl. Phys.* **83** 5025
[31] Birkl G, Kassner S and Walther H 1992 *Nature* **357** 310
[32] Lesanovsky I and von Klitzing W 2007 *Phys. Rev. Lett.* **99** 083001
[33] Rowe M A *et al* 2002 *Quantum Inf. Comput.* **2** 257
[34] Huber G, Deuschle T, Schnitzler W, Reichle R, Singer K and Schmidt-Kaler F 2008 *New J. Phys.* **10** 013004
[35] Blakestad R B, Ospelkaus C, Van Devender A P, Amini J M, Britton J, Leibfried D and Wineland D J 2009 *Phys. Rev. Lett.* **102** 153002
[36] Kaplan A, Friedman N, Andersen M and Davidson N 2001 *Phys. Rev. Lett.* **87** 274101
[37] Ryu C, Andersen M F, Clad P, Natarajan V, Helmerson K and Phillips W D 2007 *Phys. Rev. Lett.* **99** 260401
[38] Kirk D 2004 *Optimal Control Theory Introduction* (Mineda, NY: Dover)
[39] De Chiara G, Calarco T, Anderlini M, Montangero S, Lee P J, Brown L, Phillips W D and Porto J V 2008 *Phys. Rev.* A **77** 052333
[40] Singer K, Poschinger U, Murphy M, Ivanov P, Ziesel F, Calarco T and Schmidt-Kaler F 2009 arXiv:0912.0196
[41] Christandl M, Datta N, Ekert A and Landahl A J 2004 *Phys. Rev. Lett.* **92** 187902
[42] Bose S 2007 *Contemp. Phys.* **48** 13
[43] Bloch I 2008 *Science* **319** 1202
[44] Ghosh P K 1996 *Ion Traps* (Oxford: Oxford University Press)